Atmos. Chem. Phys., 16, 365–382, 2016
www.atmos-chem-phys.net/16/365/2016/
doi:10.5194/acp-16-365-2016


Atmospheric Chemistry and Physics Open Access EGU

# Global and regional emissions estimates of 1,1-difluoroethane (HFC-152a, $CH_3CHF_2$) from in situ and air archive observations

**P. G. Simmonds[1], M. Rigby[1], A. J. Manning[2], M. F. Lunt[1], S. O'Doherty[1], A. McCulloch[1], P. J. Fraser[4], S. Henne[5], M. K. Vollmer[5], J. Mühle[3], R. F. Weiss[3], P. K. Salameh[3], D. Young[1], S. Reimann[5], A. Wenger[1], T. Arnold[2], C. M. Harth[3], P. B. Krummel[4], L. P. Steele[4], B. L. Dunse[4], B. R. Miller[14], C. R. Lunder[6], O. Hermansen[6], N. Schmidbauer[6], T. Saito[7], Y. Yokouchi[7], S. Park[8], S. Li[9], B. Yao[10], L. X. Zhou[10], J. Arduini[11], M. Maione[11], R. H. J. Wang[12], D. Ivy[13], and R. G. Prinn[13]**

[1]Atmospheric Chemistry Research Group, University of Bristol, Bristol, BS8 1TS, UK
[2]Met Office Hadley Centre, Exeter, EX1 3PB, UK
[3]Scripps Institution of Oceanography (SIO), University of California San Diego, La Jolla, CA 92093, USA
[4]CSIRO Oceans and Atmosphere, Aspendale, VIC 3195, Australia
[5]Laboratory for Air Pollution and Environmental Technology, Swiss Federal Laboratories for Materials Science and Technology (Empa), Dubendorf, 8600, Switzerland
[6]Norwegian Institute for Air Research (NILU), 2027 Kjeller, Norway
[7]Centre for Environmental Measurement and Analysis, National Institute for Environmental Studies, Onogawa, Tsukuba, 305-8506, Japan
[8]Department of Oceanography, College of Natural Sciences, Kyungpook National University, Daegu, 702-701, Republic of Korea
[9]Kyungpook Institute of Oceanography, College of Natural Sciences, Kyungpook National University, Daegu, 702-701, Republic of Korea
[10]Chinese Academy of Meteorological Sciences (CAMS), Beijing, 10081, China
[11]Department of Basic Sciences and Foundations, University of Urbino, 61029 Urbino, Italy
[12]School of Earth and Atmospheric Sciences, Georgia Institute of Technology, Atlanta, Georgia, USA
[13]Center for Global Change Science, Massachusetts Institute of Technology, Cambridge, MA 02139, USA
[14]Global Monitoring Division, ESRL, NOAA, Boulder, Colorado, USA

*Correspondence to:* P. G. Simmonds (petergsimmonds@aol.com)

Received: 12 July 2015 – Published in Atmos. Chem. Phys. Discuss.: 7 August 2015
Revised: 23 November 2015 – Accepted: 1 December 2015 – Published: 18 January 2016

**Abstract.** High frequency, in situ observations from 11 globally distributed sites for the period 1994–2014 and archived air measurements dating from 1978 onward have been used to determine the global growth rate of 1,1-difluoroethane (HFC-152a, $CH_3CHF_2$). These observations have been combined with a range of atmospheric transport models to derive global emission estimates in a top-down approach. HFC-152a is a greenhouse gas with a short atmospheric lifetime of about 1.5 years. Since it does not contain chlorine or bromine, HFC-152a makes no direct contribution to the destruction of stratospheric ozone and is therefore used as a substitute for the ozone depleting chlorofluorocarbons (CFCs) and hydrochlorofluorocarbons (HCFCs). The concentration of HFC-152a has grown substantially since the first direct measurements in 1994, reaching a maximum annual global growth rate of $0.84 \pm 0.05$ ppt yr$^{-1}$ in 2006, implying a substantial increase in emissions up to 2006. However, since 2007, the annual rate of growth has slowed to $0.38 \pm 0.04$ ppt yr$^{-1}$ in 2010 with a further decline to an annual average rate of growth in 2013–2014 of $-0.06 \pm 0.05$ ppt yr$^{-1}$. The annual average Northern Hemisphere (NH) mole fraction in 1994 was 1.2 ppt rising to an annual average mole fraction of 10.1 ppt in 2014. Average annual mole fractions

in the Southern Hemisphere (SH) in 1998 and 2014 were 0.84 and 4.5 ppt, respectively. We estimate global emissions of HFC-152a have risen from $7.3 \pm 5.6$ Gg yr$^{-1}$ in 1994 to a maximum of $54.4 \pm 17.1$ Gg yr$^{-1}$ in 2011, declining to $52.5 \pm 20.1$ Gg yr$^{-1}$ in 2014 or $7.2 \pm 2.8$ Tg-$CO_2$ eq yr$^{-1}$. Analysis of mole fraction enhancements above regional background atmospheric levels suggests substantial emissions from North America, Asia, and Europe. Global HFC emissions (so called "bottom up" emissions) reported by the United Nations Framework Convention on Climate Change (UNFCCC) are based on cumulative national emission data reported to the UNFCCC, which in turn are based on national consumption data. There appears to be a significant underestimate ($> 20$ Gg) of "bottom-up" reported emissions of HFC-152a, possibly arising from largely underestimated USA emissions and undeclared Asian emissions.

## 1 Introduction

HFC-152a ($CH_3CHF_2$) is primarily sold as an aerosol and foam-blowing agent (Greally et al., 2007) and as a component of some refrigerant blends (Ashford et al., 2004). Emissions to the atmosphere show both temporal and regional variability depending on the specific application in which HFC-152a is used. Incorporation of HFC-152a into aerosol propellants results in prompt release, whereas when used as a single-component non-encapsulated blowing agent, release occurs over a period of about 2 years (McCulloch et al., 2009). Refrigerant use of HFC-152a results in release over longer periods, possibly up to 20 years. Reported emissions of HFC-152a are likely to be incomplete as a consequence of a limited number of producers and confidentiality considerations. Emissions of HFC-152a for some countries are aggregated with other hydrofluorocarbons (HFCs) in a category reported to the UNFCCC as "unspecified mix". For example, emissions reported by the USA to the UNFCCC for HFC-152a, 227ea, 245ca and 43-10mee are shown in the database as "commercially confidential", and they constitute the aggregated "unspecified" emissions. HFC-152a emissions from the USA are estimated to be the primary contributor to the total for this gas from Annex 1 countries (Lunt et al., 2015). Previous papers (Manning and Weiss, 2007; Millet et al., 2009; Stohl et al., 2009; Barletta et al., 2011; Miller et al., 2012; Simmonds et al., 2015) have reported major differences between USA HFC-152a emission estimates derived from atmospheric measurements (top down) and emissions calculated from US reports to the UNFCCC (bottom up). The apparent under-reporting of USA emissions to the UNFCCC ranges from 20–60 Gg based on annual average estimates.

HFC-152a has the smallest 100-year global warming potential ($GWP_{100}$, 138) of all the major HFCs (Forster et al., 2007; Myhre et al., 2013), with a short atmospheric lifetime of 1.5 years, due to efficient reaction with tropospheric hydroxyl (OH) radicals (SPARC Report No. 6, 2013). Unlike hydrocarbons, HFC-152a does not participate in the reaction to form ozone in the troposphere. These desirable properties have made HFC-152a especially attractive as a replacement, not only for CFCs (chlorofluorocarbons) and HCFCs (hydrochlorofluorocarbons), but also increasingly for HFC-134a in technical aerosol applications and mobile air-conditioners (IPCC/TEAP, 2011).

Ryall et al. (2001) using observations from Mace Head, Ireland reported the distribution of European HFC-152a emissions, concentrated in Germany, and estimated an average European total emission of 0.48 Gg yr$^{-1}$ for 1995–1998. Reimann et al. (2004) used a 3-year data set (2000–2002) of HFC-152a observations at the Swiss Alpine station Jungfraujoch and trajectory modeling, also noting a predominantly German source for European HFC-152a emissions. This group measured an atmospheric growth rate of 0.3 ppt yr$^{-1}$ (ppt – parts per trillion, $10^{-12}$, mol mol$^{-1}$ or pmol mol$^{-1}$) from 2000 to 2002 and a December 2002 mole fraction at the Jungfraujoch station of 3.2 ppt, from which they estimated a European emission strength of 0.8 Gg yr$^{-1}$ for 2000–2002.

In the Southern Hemisphere HFC-152a monthly means, annual means and trends have been reported from observations at Cape Grim, Tasmania, for 1998–2004 (Sturrock et al., 2001; Fraser et al., 2014a; Krummel et al., 2014). The HFC-152a annual means have grown from 0.8 ppt (0.1 ppt yr$^{-1}$) in 1998 to 1.8 ppt (0.4 ppt yr$^{-1}$) in 2004. More recent estimates of SE Australian HFC-152a emissions (2005–2012) have been calculated by interspecies correlation and model inversions and by extrapolation based on population (Fraser et al., 2014a).

Here we further expand the HFC-152a record up to the end of 2014 using in situ observations from 11 globally distributed monitoring stations (9 Advanced Global Atmospheric Gases Experiment (AGAGE) stations and 2 affiliated stations), together with atmospheric transport models to independently estimate HFC-152a emissions on regional and global scales. We then compare these with HFC-152a emission estimates compiled from national reports to the United Nations Framework Convention on Climate Change (UNFCCC) and Emissions Database for Global Atmospheric Research (EC-JRC/PBL EDGAR v4.2; http://edgar.jrc.ec.europa.eu/), using the same techniques reported for other greenhouse gases (O'Doherty et al., 2009, 2014; Miller et al., 2010; Vollmer et al., 2011; Krummel et al., 2014; Rigby et al., 2014).

## 2 Experimental methods

### 2.1 Instrumentation and calibration

High frequency, in situ measurements of HFC-152a were made by gas chromatography-mass spectrometry (GC-Agilent 6890) coupled with quadrupole mass selective detec-

tion (MSD-Agilent 5973/5975). Measurements commenced at Mace Head, Ireland in 1994 and Cape Grim, Tasmania in 1998, using a custom-built automated pre-concentration system (adsorption desorption system – ADS) to selectively and quantitatively retain halogenated compounds from 2 L air samples. Based on a Peltier–cooled pre-concentration microtrap cooled to −50 °C during the adsorption phase, the ADS provided on-site calibrated air samples every 4 h, i.e., six per day (Simmonds et al., 1995). In 2004, the ADS-GC-MS was replaced with a more advanced custom-built pre-concentration system (Medusa) with enhanced cooling to ∼ −180 °C and the relatively mild adsorbent HayeSep D (Miller et al., 2008; Arnold et al., 2012). Agilent 5973 MSDs (mass selective detector) were also upgraded to the Agilent 5975 MSDs over the course of the Medusa observations. Analysis of each 2 L sample of ambient air was alternated with analysis of a 2 L reference gas (designated as a working standard) to correct for short-term instrumental drift, resulting in 12 (Medusa) individually calibrated air measurements per day. Working standards were prepared for each station by compressing ambient air into 34 L electropolished stainless steel canisters (Essex Industries, Inc., Missouri) using modified oil-free compressors (SA-6, RIX, California). Exceptions to this were the Cape Grim and Zeppelin stations, where the working standards were filled using a cryogenic filling technique. Research-grade helium, which was used as a carrier gas in the Medusa systems, was further purified by passage through a heated "getter" type purifier (Valco Instruments, Houston, TX). The carrier gas was analyzed for blanks on a regular basis and blank levels of HFC-152a were below the limit of detection at all field stations.

Table 1 lists the geographical location and the time when routine ambient measurements of HFC-152a began at each monitoring station. Stations with the longest observational records that deployed both ADS and Medusa GC-MS instruments include Mace Head (MHD), Jungfraujoch (JFJ), Ny-Ålesund (ZEP) and Cape Grim (CGO). Medusa GC-MS instruments were installed at five other AGAGE stations Trinidad Head (THD), Gosan (GSN), Ragged Point, (RPB), Shangdianzi (SDZ), and Cape Matatula (SMO) between 2003 and 2010. In addition two AGAGE affiliated stations Monte Cimone (CMN) and Hateruma (HAT), which use comparable GC-MS instruments, but a different pre-concentration design for sample enrichment, commenced HFC-152a measurements in 2001 and 2004, respectively. Importantly, all 11 stations listed in Table 1 report HFC-152a measurements relative to the Scripps Institution of Oceanography (SIO-05) calibration scale (as dry gas mole fractions in pmol $mol^{-1}$).

The estimated accuracy of the calibration scale for HFC-152a is 4 %: a more detailed discussion of the measurement technique and calibration procedure is reported elsewhere (Miller et al., 2008; O'Doherty et al., 2009; Mühle et al., 2010). HFC-152a was determined using the MS in selected ion monitoring mode (SIM) with a target ion $CH_3CF_2^+$ ($m/z$ 65) and qualifier ion $CH_3CF^+$ ($m/z$ 46). To ensure that potential interferences from co-eluting species did not compromise the analysis, the ratio of the target to qualifier ion was continuously monitored. Measurement precision was calculated as the daily standard deviation ($1\sigma$) of the ratios of each standard response to the average of the closest-in-time preceding and subsequent standard responses. Typical daily precisions vary from station to station with a range of 0.1–0.4 ppt. Individual station precisions were used to estimate the precision of each in situ measurement.

### 2.2 Northern and Southern Hemisphere archived air samples

In order to extend the HFC-152a data record back before the commencement of high-frequency measurements, analyses of Northern Hemisphere (NH) and Southern Hemisphere (SH) archived air samples dating back to 1978, were carried out using three similar Medusa GC-MS instruments at the Scripps Institution of Oceanography (SIO), La Jolla, California, the Commonwealth Scientific and Industrial Research Organisation (CSIRO), Aspendale, Australia and the Cape Grim Baseline Air Pollution Station, Tasmania. The SH samples are part of the Cape Grim air archive (CGAA) described in Langenfelds et al. (1996), and Krummel et al. (2007). The NH samples analyzed for this paper were filled during background conditions mostly at Trinidad Head, but also at La Jolla, California; Cape Meares, Oregon; Ny Ålesund, Svalbad and Point Barrow, Alaska (some samples are courtesy of the National Oceanic and Atmospheric Administration (NOAA).

In addition, eight SH samples were measured at SIO and compared with SH samples of similar age measured at CSIRO (February 1995, July 1995, November 1995, June 1998, July 2004, February 2006, August 2008, and December 2010, $\Delta x = 0.01$–$0.07$ ppt $\Delta t = 1$–$33$ days) and three NH samples were measured at CSIRO and compared with NH samples of the same age measured at SIO (May 1989 and April 1999, $\Delta x = 0.02$–$0.06$ ppt, $\Delta t = 1$–11 days). The good agreement between SIO and CSIRO archived air stored in different types of tanks (stainless steel tanks, Essex Industries, Inc and Silcosteel treated tanks, Restek Corporation) serves both as proof of the good consistency of the individual Medusa GC-MS instruments and the integrity of the tanks used. Samples were analyzed in replicate typically 3–6 times each and several NH tanks were re-measured over a number of years.

### 2.3 Selection of baseline data

Baseline in situ monthly mean HFC-152a mole fractions were calculated by excluding values enhanced by local and regional pollution influences, as identified by the iterative AGAGE pollution identification algorithm, (see Appendix in O'Doherty et al., 2001). Briefly, baseline measurements

**Table 1.** Overview of the 11 measurement stations used in this study, their coordinates and periods for which data are available.

| Station | Latitude | Longitude | ADS data* | Medusa data** |
|---|---|---|---|---|
| Ny-Ålesund, Norway[a] | 78.9° N | 11.9° E | 2001–2010 | September 2010–present |
| Mace Head, Ireland[a] | 53.3° N | 9.9° W | 1994–2004 | June 2003–present |
| Jungfraujoch, Switzerland[a] | 46.5° N | 8.0° E | 2000–2008 | May 2008–present |
| Monte Cimone, Italy[b] | 44.2° N | 10.7° E | | June 2001–present[b] |
| Trinidad Head, California[a] | 41.0° N | 124.1° W | | March 2005–present |
| Shangdianzi, China[a,c] | 40.4° N | 117.7° E | | May 2010–August 2012 |
| Gosan, Jeju Island, Korea[a] | 33.2° N | 126.2° E | | November 2007–present |
| Hateruma, Japan[b] | 21.1° N | 123.8° E | | May 2004–present[b] |
| Ragged Point, Barbados[a] | 13.2° N | 59.4° W | | May 2005–present |
| Cape Matatula, Samoa[a] | 14.2° S | 170.6° W | | May 2006–present |
| Cape Grim, Tasmania[a] | 40.7° S | 144.7° E | 1998–2004 | Jan 2004–present |

[a] AGAGE stations; [b] Affiliated stations use a different pre-concentration system (non-Medusa) than the AGAGE stations, but comparable GC-MS analytical instruments (see Yokouchi et al., 2006; Maione et al., 2014). [c] Shangdianzi was only operational for a short period and is not included in the modeling studies. * Period of HFC-152a data record using ADS-GC-MS. ** Period of HFC-152a data record using Medusa-GC-MS.

are assumed to have a Gaussian distribution around the local baseline value, and an iterative process is used to filter out the points that do not conform to this distribution. A second-order polynomial is fitted to the subset of daily minima in any 121-day period to provide a first estimate of the baseline and seasonal cycle. After subtracting this polynomial from all the observations a standard deviation and median are calculated for the residual values over the 121-day period. Values exceeding 3 standard deviations above the baseline are thus identified as non-baseline (polluted) and removed from further consideration. The process is repeated iteratively to identify and remove additional non-baseline values until the new and previous calculated median values agree within 0.1 %. For the core AGAGE stations, in situ baseline data and archive air data, extending the record to periods prior to the in situ measurement period, are then combined for each hemisphere, and outliers are rejected by an iterative filter.

## 3 Modeling studies

We pursued several approaches to determine emissions at global, continental and regional scales. The methodologies have been published elsewhere and are summarized below. The global, continental and some regional estimates incorporate a priori estimates of emissions, which were subsequently adjusted using the observations.

There are several sources of information on production and emissions of HFC-152a; none of which, on their own, provides a complete database of global emissions. The more geographically comprehensive source of information is provided by the parties to the UNFCCC, but only includes Annex 1 countries (developed countries). The 2014 database covers years 1990 to 2012 and are reported in Table 2(II) s1 in the common reporting format (CRF) available at http://unfccc.int/national_reports/annexighginventories/nationalinventoriessubmissions/items/8108.php. An alternative inventory estimate was also obtained from the Emissions Database for Global Atmospheric Research (EDGAR v4.2; http://edgar.jrc.ec.europa.eu/), a database that estimates global emission inventories of anthropogenic greenhouse gases (GHGs) on a country, region and grid basis up to 2008.

To infer "top-down" emissions we select observations from the various observing sites listed in Table 1 and four chemical transport models. These 11 sites are sensitive to many areas of the world in which HFC-152a emissions are reported; however, other areas of the globe that are not well monitored by this network are also likely to have significant emissions (such as South Asia, South Africa, and South America).

### 3.1 Global emissions estimates using the AGAGE two-dimensional 12-box model

To estimate global-average mole fractions and derive growth rates, a two-dimensional model of atmospheric chemistry and transport was employed. The AGAGE 12-box model simulates trace gas transport in four equal mass latitudinal sections (divisions at 30–90° N, 0–30° N, 30–0° S and 90–30° S) and at three heights (vertical divisions at 200, 500 and 1000 hPa). The model was originally developed by Cunnold et al. (1983) (nine-box version), with subsequent improvements by Cunnold et al. (1994) and Rigby et al. (2013, 2014). Emissions were estimated between 1989 and 2014 using a Bayesian method in which an a priori constraint (EDGAR v4.2) on the emissions growth rate was adjusted using the baseline-filtered AGAGE observations (Rigby et al., 2011a, 2014). Global emissions were derived that included estimates of the uncertainties due to the observations, the prior and the lifetime of HFC-152a, as detailed in the supplementary material in Rigby et al. (2014). Note that historically and here the

**Table 2.** Estimates of global emissions of HFC-152a ($Gg\,yr^{-1} \pm 1\sigma$) based on AGAGE in situ measurements using the AGAGE 2-D 12-box model. Emission inventories as reported in UNFCCC (United Nations Framework Convention on Climate Change) National Inventory Reports (DoE, 2014; National Inventory Report 2012, submission), EDGAR (v4.2) database and recalculated from the UNFCCC data as described in the text.

| Year | AGAGE ($Gg\,yr^{-1}$) | UNFCCC as reported ($Gg\,yr^{-1}$) | EDGAR (4.2) ($Gg\,yr^{-1}$) | UNFCCC including "unspecified" contribution ($Gg\,yr^{-1}$) |
|---|---|---|---|---|
| 1994 | $7.3 \pm 5.6$ | | | |
| 1995 | $7.9 \pm 7.4$ | 1.0 | 7.3 | 8.8 |
| 1996 | $9.1 \pm 8.4$ | 1.1 | 8.9 | 13.3 |
| 1997 | $11.3 \pm 8.6$ | 1.3 | 10.3 | 15.4 |
| 1998 | $12.5 \pm 10.9$ | 1.2 | 11.7 | 13.3 |
| 1999 | $14.4 \pm 11.2$ | 1.4 | 13.2 | 14.0 |
| 2000 | $16.6 \pm 12.2$ | 2.2 | 15.2 | 13.0 |
| 2001 | $18.4 \pm 13.4$ | 3.5 | 15.9 | 15.4 |
| 2002 | $22.5 \pm 14.7$ | 4.5 | 18.6 | 17.6 |
| 2003 | $26.3 \pm 15.3$ | 4.7 | 20.6 | 17.7 |
| 2004 | $29.2 \pm 15.6$ | 4.8 | 21.7 | 18.1 |
| 2005 | $35.8 \pm 14.7$ | 4.3 | 23.0 | 16.5 |
| 2006 | $43.3 \pm 14.9$ | 4.4 | 24.9 | 16.7 |
| 2007 | $48.1 \pm 17.6$ | 4.4 | 26.4 | 16.8 |
| 2008 | $48.9 \pm 16.7$ | 4.3 | 28.0 | 16.4 |
| 2009 | $48.0 \pm 16.4$ | 4.6 | | 17.6 |
| 2010 | $53.4 \pm 17.5$ | 4.9 | | 18.6 |
| 2011 | $54.4 \pm 17.1$ | 5.0 | | 19.3 |
| 2012 | $53.2 \pm 18.5$ | 5.2 | | 20.5 |
| 2013 | $52.5 \pm 17.8$ | | | |
| 2014 | $52.5 \pm 20.1$ | | | |

12-box model only uses observations from the core AGAGE sites, Mace Head, Trinidad Head, Ragged Point, Cape Matatula, and Cape Grim.

### 3.2 Global and continental emissions estimates using a combined Eulerian and Lagrangian model

We used the methodology outlined in Lunt et al. (2015) and Rigby et al. (2011b) to derive emissions of HFC-152a from continental regions. The high-resolution, regional UK Met Office Numerical Atmospheric-dispersion Modelling Environment (NAME), Manning et al. (2011) was used to simulate atmospheric HFC transport close to a subset of AGAGE monitoring sites, which were strongly influenced by regional HFC sources (domains shown by red boxes in Fig. 1). Simultaneously, the influence of changes to the global emissions field on all measurement stations was simulated using the global Model for OZone and Related Tracers, MOZART (Emmons et al., 2010). We estimated annual emissions for the period 2007–2012 and aggregated the derived emissions fields into continental regions, separating countries that either do ("Annex-1"), or do not ("non-Annex-1") report detailed, annual emissions to the UNFCCC. Emissions were estimated using a hierarchical Bayesian inverse method (Ganesan et al., 2014; Lunt et al., 2015) and all high-frequency observations from 10 of the 11 sites listed in Table 1, excluding Shangdianzi due to the short time series. The hierarchical Bayesian method includes uncertainty parameters (e.g., model "mismatch" errors and a priori uncertainties) in the estimation scheme, reducing the influence of subjective choices on the outcome of the inversion.

### 3.3 High-resolution regional emissions estimates using InTEM

A method for estimating emissions from observations and atmospheric transport modeling with NAME referred to as InTEM, "Inversion Technique for Emission Modelling" (Manning et al., 2011), uses a simulated annealing method (Press et al., 1992) to search for the emission distribution that produces a modeled times series that has the best statistical match to the observations from certain AGAGE stations (e.g., Mace Head, Cape Grim). NAME was driven with output from the operational analysis of the UK Met Office Numerical Weather Prediction model, the Unified Model, at global horizontal resolution of 17–40 km (year dependent). InTEM estimates the spatial distribution of emissions across a defined geographical area, and can either start from a random emission distribution or be constrained by an inventory-defined distribution. Emission totals from specific geographical areas are calculated by summing the derived emissions from each grid (non-uniform) in that region.

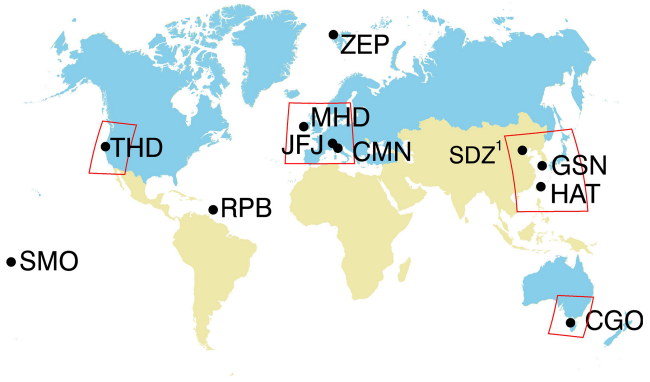


**Figure 1.** Location of AGAGE and affiliated stations. Ny-Ålesund, Zeppelin, Norway (ZEP); Mace Head, Ireland (MHD); Jungfraujoch, Switzerland (JFJ); Monte Cimone, Italy (CMN); Trinidad Head, USA (THD); Shangdianzi, China (SDZ); Gosan, South Korea (GSN); Hateruma, Japan (HAT); Ragged Point, Barbados (RPB); Cape Matatula, American Samoa (SMO); and Cape Grim, Tasmania (GCO). Red boxes indicate "local regions" where the NAME model was used with increased resolution compared to the global MOZART model, Annex 1 countries are shaded blue and non-Annex 1 countries are shaded yellow. Note: [1] Shangdianzi (SDZ) was not used in any of the modeling studies due to the relatively short time series.

The uncertainty estimation used within InTEM is described in detail elsewhere (Manning et al., 2011). Briefly, the uncertainty space was explored by (a) solving the inversion multiple times with a range of baseline mole fractions within the baseline uncertainty estimated during the baseline fitting process and (b) by altering the 3-year inversion time window by 1 month throughout the data period thereby solving over a particular 1-year period many times using different observations. In total for each annual estimate, up to 111 inversions were performed; the median and 5th and 95th percentiles were used as the final total and spread. For the Australian estimates data between 2002 and 2011 were used, for the NW European estimates data between November 1994 and December 2013 were used.

### 3.4 High-resolution European emission estimates using the FLEXPART model

A regional Bayesian inversion system using backward simulations of a Lagrangian particle dispersion model FLEXPART (Stohl et al., 2005) was applied to the HFC-152a observations from Mace Head, Jungfraujoch and Mt. Cimone for the period 2006 to 2014. The inversion technique follows the description by Stohl et al. (2009) and was previously applied to regional halocarbon emissions from Europe (Keller et al., 2012; Maione et al., 2014) and China (Vollmer et al., 2009). For these emission estimates, the background was determined by applying the Robust Extraction of Baseline Signal (REBS) filter described in detail by Ruckstuhl et al. (2012). The transport model FLEXPART was driven with output from the operational analysis of the Integrated Forecast System (IFS) of the European Centre for Medium Range Weather Forecast (ECMWF) using a spatial resolution of $0.2° \times 0.2°$ for a nested domain covering the larger area of the European Alps and a spatial resolution of $1° \times 1°$ elsewhere.

The FLEXPART model was applied to the HFC-152a observations from Mace Head, Jungfraujoch and Mt. Cimone for the period 2006 to 2014. Prior to 2006, the model resolution of Integrated Forecast System (IFS) was not sufficiently fine to realistically simulate the transport to the two high altitude sites Jungfraujoch and Mt. Cimone. Therefore, no attempt was made here to apply the inversion system to years before 2006. As prior information of the HFC-152a emissions we used country totals as submitted to UNFCCC. These were spatially disaggregated following the HFC-152a distribution given in EDGAR (v4.2). For countries not reporting HFC-152a emissions to UNFCCC we used the values given in EDGAR. The EDGAR inventory was only available up to the year 2008 beyond this year the EDGAR 2008 distribution was used. The uncertainty of the prior emissions was set so that the region total uncertainty equalled 20 % of the region total emissions. The regional inversion grid covered a region similar to that shown in Fig. 1.

### 3.5 Regional emissions estimates using the inter-species correlation (ISC) methods

We also present regional emissions estimates using inter-species correlation (ISC) methods (Yokouchi et al., 2005). Emissions of a number of trace gases from the Melbourne/Port Phillip region (CFCs, HCFCs, HFCs, carbon tetrachloride: Dunse et al., 2001, 2002, 2005; O'Doherty et al., 2009; Fraser et al., 2014a, b), including HFC-152a (Greally et al., 2007), have been estimated utilizing in situ high frequency measurements from Cape Grim and ISC with co-incident carbon monoxide (CO) measurements.

ISC works best for co-located sources – however extensive modeling has shown that by the time the Melbourne/Port Phillip plume reaches Cape Grim (300 km from the source) it is well mixed and the likely inhomogeneity of the source regions (for CO and HFC-152a in this case) does not have a significant influence on the derived emissions. It should be noted that in order to obtain a significant sampling of Port Phillip pollution episodes at Cape Grim, data from 3 years (for example 2011–2013) are used to derive annual emissions (for 2012). (InTEM also uses data from 3 years to derive annual emissions.) The ISC uncertainties given in the paper include (1) the uncertainties in the estimates of CO emissions from Melbourne/Port Phillip (2) the uncertainties in the overall correlation between CO and HCFC-152a as seen in pollution episodes at Cape Grim (3) the uncertainties in the geographic extent of the HFC-152a and CO source regions impacting on Cape Grim and their entrained population.

Using HCFC-22 as the reference tracer, Li et al. (2011) reported that China is the dominant emitter of halocarbons in East Asia. North American HFC-152a emissions have been estimated from atmospheric data using interspecies correlation based techniques with CO (Millet et al., 2009; Barletta et al., 2011) and fossil fuel $CO_2$ (Miller et al., 2012) as the reference emissions.

## 4 Results and discussion

### 4.1 In situ observations

The time series of HFC-152a in situ observations recorded at selected AGAGE and affiliated monitoring stations are shown in Fig. 2a–c. Data have been filtered into baseline (black) and above baseline (red) using the AGAGE pollution algorithm, as discussed in Sect. 2.3. Figure 2a shows the mole fractions in ppt for the four stations that deployed both ADS and Medusa GC-MS instruments (Mace Head, Zeppelin, Jungfraujoch, and Cape Grim). Most notable are the substantial above baseline events at Mace Head and Jungfraujoch that are influenced primarily by emissions from European sources. Conversely, the Zeppelin Arctic station and the SH station at Cape Grim have relatively small above baseline events implying smaller emissions from local or regional sources.

Figure 2b shows measurements at the five other AGAGE stations (Trinidad Head, Gosan, Ragged Point, Shangdianzi, and Cape Matatula), which used only Medusa GC-MS instruments. The North American site at Trinidad Head and the Asian sites at Shangdianzi and Gosan are the most strongly influenced by regional emissions. The tropical sites at Ragged Point, Barbados, and Cape Matatula, American Samoa show very few enhancements above the baseline and these are due mostly to local emissions occurring under nighttime inversion conditions and occasional influences from regional emission sources (note the different *y* axis scales). Although the Shangdianzi station was operational for only a short period, the enhancements above baseline are significant due to the sensitivity of this site to Chinese emissions, and comparable in magnitude to those at Gosan.

Figure 2c illustrates the time series from the two affiliated AGAGE stations (Monte Cimone and Haturuma) that used comparable GC-MS instruments but with different methods of pre-concentration. Monte Cimone, like the Jungfraujoch, is also influenced by substantial emissions from sources in continental Europe. Hateruma is influenced by sources in China, Korea, Taiwan, and Japan (Yokouchi et al., 2006).

### 4.2 Atmospheric trends and seasonal cycles

Figure 3 shows the in situ measurements of HFC-152a, as baseline monthly means (excluding pollution events), obtained from the two AGAGE stations Mace Head and Cape Grim with the longest time series that deployed both ADS and Medusa GC-MS instruments. Superimposed in Fig. 3 are the NH and SH archived flask data extending back to 1978. Annual average mole fractions at Mace Head increased from 1.2 ppt in 1994 to 10.2 ppt by 2014, Cape Grim annual average mole fractions increased from 0.84 ppt in 1998 when in situ measurements first began to 4.5 ppt in 2014. However, in the last few years the rates of growth at both sites have slowed to almost zero.

The NH archived samples are more variable than the SH archived samples. The SH archive is collected only under strict baseline conditions (Southern Ocean air) and is far removed from the major sources of HFC-152a. Conversely in the NH, where most major sources of emissions are located, sampling under strict baseline conditions is more difficult to achieve.

Figure 4a illustrates HFC-152a baseline monthly means obtained from the five other AGAGE observing sites (Ragged Point, Gosan, Cape Matatula, Trinidad Head, and Shangdianzi using only the more advanced Medusa GC-MS. There is a large seasonal cycle at Gosan with a very deep minimum due to summertime transport from the Southern Hemisphere (Li et al., 2011). Barbados can also be influenced by Southern Hemispheric air during the hurricane season (Archibald et al., 2015).

Figure 4b shows the baseline monthly mean mole fractions for the three mountain stations. Ny-Ålesund and Jungfraujoch, using combined ADS and Medusa GC-MS measurements and Monte Cimone, which used a commercial preconcentrator GC-MS. In most years Monte Cimone exhibits enhanced mole fractions during the NH spring months (March–May).

The HFC-152a seasonal cycles at Mace Head and Cape Grim shown in Fig. 5a and b, are broadly representative of the Northern Hemisphere and Southern Hemisphere, respectively. The seasonal cycle at Mace Head shows a NH spring maximum (April–May) and late summer minimum (August–October), while the SH seasonal cycle at Cape Grim exhibits a broad austral spring maximum (July–November) and a late summer minimum (January–April). The summer minimum at both locations is attributed to enhanced summertime loss (OH) with possibly a contribution from seasonally varying emissions in the NH that may be out-of-phase with the NH sink. At Cape Grim an additional source of seasonality is due to seasonally varying transport between the NH and SH, which is generally in phase with the sink induced seasonal cycle. This competition between OH summertime loss and seasonally varying transport has been observed at many other AGAGE locations (Prinn et al., 1992; Greally et al., 2007; O'Doherty et al., 2009, 2014; Li et al., 2011).

Figure 6 shows the mole fractions output from the AGAGE global 12-box model, along with the monthly mean semi-hemispheric average observations used in the inversion. The figure also shows the running mean growth rate, smoothed using a Kolmogorov–Zurbenko filter with a window of approximately 12 months (Rigby et al., 2014). Most notable

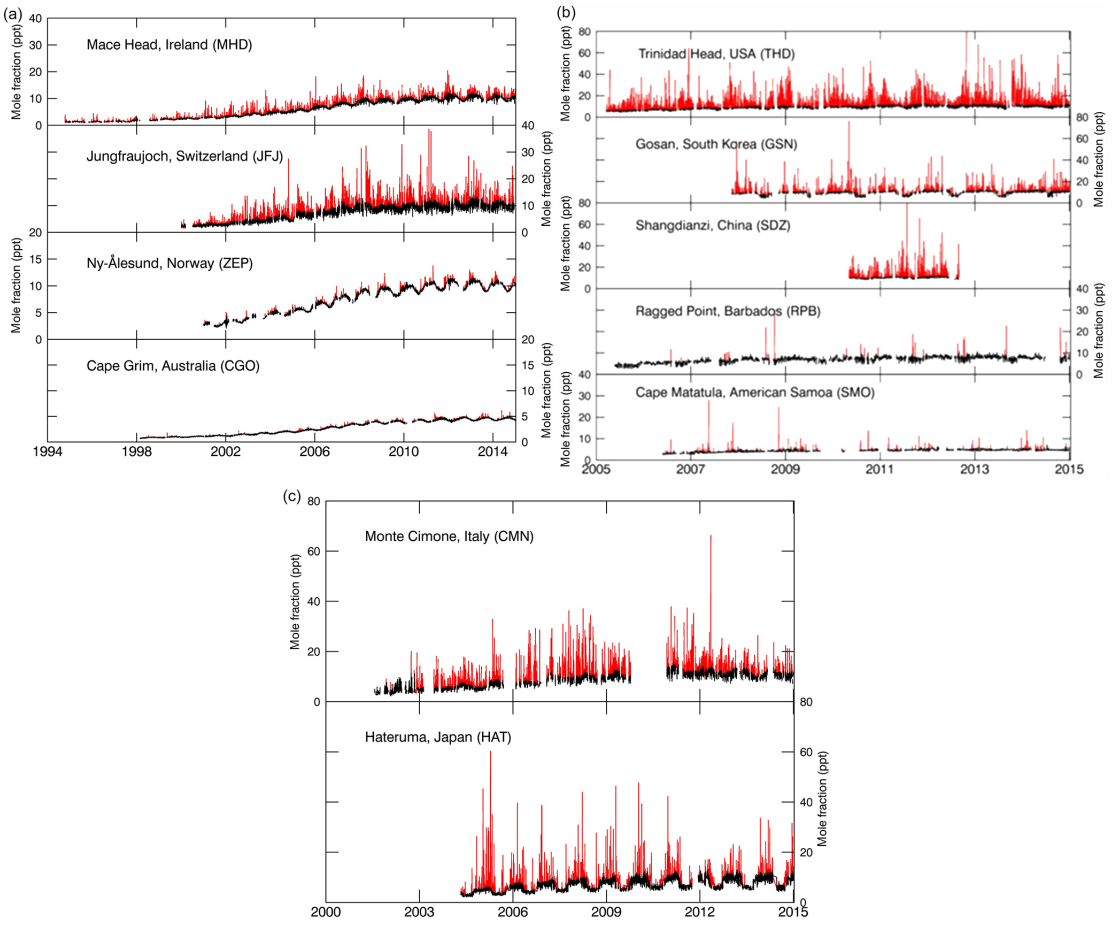


**Figure 2. (a)** Time series of HFC-152a mole fractions (ppt) recorded at the four monitoring stations with combined ADS and Medusa data. (MHD, JFJ, ZEP and CGO), (note the different $y$ axis scales). Data have been assigned as baseline (black) and non-baseline (red) using the AGAGE pollution identification algorithm. **(b)** Time series of HFC-152a mole fractions (ppt), recorded with the Medusa GC-MS instruments at the five AGAGE monitoring stations (THD, GSN, SDZ, RPB, and SMO). Data have been assigned as baseline (black) and non-baseline (red) using the AGAGE pollution identification algorithm. **(c)** Time series of HFC-152a mole fractions (ppt) recorded with the GC-MS instruments at the two affiliated AGAGE stations CMN and HAT. Data have been assigned as baseline (black) and non-baseline (red) using the AGAGE pollution identification algorithm.

is the positive growth rate from 1995 reaching a maximum of $\sim 0.84$ ppt yr$^{-1}$ in 2006, followed by a steady decline in the growth rate with a minimum during the economic recession in 2008–2009. The positive growth rate then resumes increasing to $\sim 0.4$ ppt yr$^{-1}$ in 2010 followed by a subsequent decrease with an annual average growth rate in 2013–2014 of minus $\sim 0.06$ ppt yr$^{-1}$.

The strong inter-hemispheric gradient demonstrates that emissions are predominantly in the NH, as has been illustrated for many other purely anthropogenic trace gases (Prinn et al., 2000). The globally averaged mole fraction in the lower troposphere in 2014 is estimated to be $6.84 \pm 0.23$ ppt and the annual rate of increase is $-0.06 \pm 0.05$ ppt yr$^{-1}$. As reported by Rigby et al. (2014) the major long lived synthetic greenhouse gases (SGHGs) which include CFCs, HCFCs, HFCs, and perfluorocarbons ($SF_6$ and $NF_3$), as well as $CH_3CCl_3$ and $CCl_4$ were responsible for $350 \pm 10$ mW m$^{-2}$ of direct radiative forcing in 2012. The radiative forcing of HFC-152a, determined from the AGAGE 12-box model in this study, was $0.61 \pm 0.02$ mW m$^{-2}$ in 2014, which represents only a tiny fraction ($\sim 0.2$ %) of the global radiative forcing of the SGHG.

## 5 Top-down emission estimates

### 5.1 Global estimates

Estimated global emissions of HFC-152a using the 12-box model and the reported UNFCCC and EDGAR emission inventories are shown in Fig. 7 and Table 2. The blue solid line represents our model-derived emissions, with the $1\sigma$ error band shown by the shaded areas. Model derived emissions

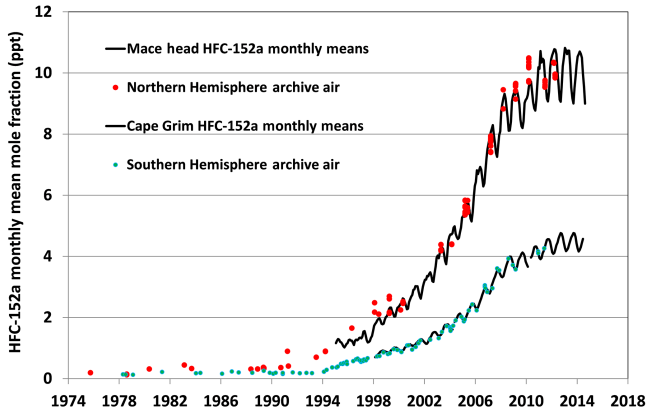


**Figure 3.** HFC-152a baseline monthly mean mole fraction (ppt) recorded at Mace Head-MHD (ADS GC-MS, 1994–2003; Medusa GC-MS, 2004–2014) and at Cape Grim-CGO (ADS GC-MS, 1998–2003; Medusa GC-MS, 2004–2014) and from analysis of archived NH and SH air samples extending back to 1975: in situ (black), air archive NH (red) and SH (blue).

grew steadily from 1995 to 2007 with a non-statistically significant decrease in emissions in 2009 to $48 \pm 16.4$ Gg yr$^{-1}$, during the economic downturn in 2008–2009. The mean emission reached a maximum of $54.4 \pm 17.1$ Gg yr$^{-1}$ in 2011, followed by a period of relatively stable emissions, the mean showing a slight decline to $52.5 \pm 20.1$ Gg yr$^{-1}$ ($7.2 \pm 2.8$ Tg-$CO_2$ eq yr$^{-1}$) in 2014.

The data shown in column 3 of Table 2 are the totals of submissions by the national governments to the UNFCCC (Rio Convention) as reported in Table 2(II) s1 in the Common Reporting Format (CRF), available on the UNFCCC website (http://unfccc.int/nationalreports/annexighginventories/nationalinventoriessubmissions/items/8108.php). The values were taken from the 2014 database and cover years 1995 (the baseline year for submissions) to 2012. In addition to reporting calculated emissions of HFCs 23, 32, 125, 134a, 143a, 152a, 227ea, 236fa, 245ca, and 43-10mee individually, many countries also included "unspecified" emissions in this database (as the sum of their $CO_2$ equivalents). Where the unspecified component was small in relation to the national specified emissions, it was disaggregated by assuming that it had the same fractional contribution of each HFC as reported in the specified components (adjusted for their $CO_2$ equivalence). However, in the US, although values of emissions of several HFCs are calculated specifically for the individual substances, HFCs 152a, 227ea, 245ca and 43-10mee are shown in the database as "commercially confidential" and their emissions apparently constitute the substantial aggregated "unspecified" emissions reported. Hence, for the US, these unspecified annual emissions were divided only between HFCs 152a, 227ea, 245ca and 43-10mee, assuming the same ratio as their reported global emissions, all expressed as $CO_2$ equivalents. The values shown in column 4 of Table 2 are the global totals of HFC-152a after adjusting in these ways for the quantities included in "unspecified" emissions.

The additional component of US emissions makes a substantial contribution to the very large difference between the UNFCCC data as reported and the adjusted values. This is partly due to the low global warming potential of HFC-152a (a factor of 10 lower than other HFCs) which magnifies its mass component in the 8200 Gg $CO_2$ equivalent of US "unspecified" emissions.

The AGAGE observation based global emissions are substantially higher than the emissions calculated from the UNFCCC GHG reports (2014 submission). It is not unreasonable that UNFCCC-reported emissions are lower than the AGAGE global emission estimates, since countries and regions in Asia (e.g., China, Indonesia, Korea, Malaysia, the Philippines, Taiwan, Vietnam), the Indian sub-continent (e.g., India, Pakistan), the Middle East, South Africa, and Latin America do not report to the UNFCCC. Where we include the HFC-152a component of unspecified emissions (green line in Fig. 7) results are consistent within the error bars until approximately 2003 to 2005 when they start to diverge (UNFCCC + "unspecified" lower). From 1996 to 2002, estimated emissions from EDGAR (v4.2) are generally consistent with AGAGE emissions, but then begin to diverge with EDGAR emissions 22 Gg below 2008 AGAGE emissions, the last year for which EDGAR reports emissions.

### 5.2 Regional emissions of HFC-152a inferred for Europe, United States, Asia, and Australia

Lunt et al. (2015) have reported global and regional emissions estimates for the most abundant HFCs, based on inversions of atmospheric mole fraction data, aggregated into two categories; those from Annex 1 countries and those from non-Annex 1 countries. The inversion methodology used the NAME model to simulate atmospheric transport close to the monitoring sites, and the Model for Ozone and Related chemical Tracers (MOZART, Emmons et al., 2010) to simultaneously calculate the effect of changes to the global emissions field on each measurement site. The model sensitivities were combined with a prior estimate of emissions (based on EDGAR) and the atmospheric measurements, in a hierarchical Bayesian inversion (Ganesan et al., 2014), to infer emissions.

Using this method we infer emissions estimates for the entire world, Europe, North America, and East Asia. Table 3 lists our estimated regional emissions in Gg yr$^{-1}$ averaged across two time periods: 2007–2009 and 2010–2012, together with our global emission estimates averaged over the same time periods from the 12-box model. It is apparent that North American average annual emissions ($\sim 30$ Gg) are the major contributor to the global total with Europe contributing annual average emissions from about 5–6 Gg yr$^{-1}$. East Asia

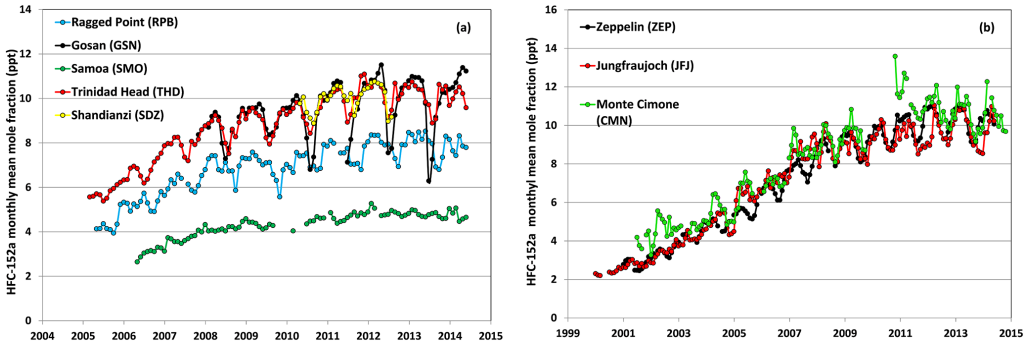


**Figure 4. (a)** Medusa GC-MS baseline monthly mean mole fractions (ppt) recorded at Ragged Point, Gosan, Cape Matatula, Trinidad Head, and Shangdianzi. Observations at Shangdianzi were discontinued in August 2012. **(b)** Combined ADS and Medusa GC-MS baseline monthly mean mole fraction recorded at Ny-Ålesund, Jungfraujoch, and Monte Cimone.

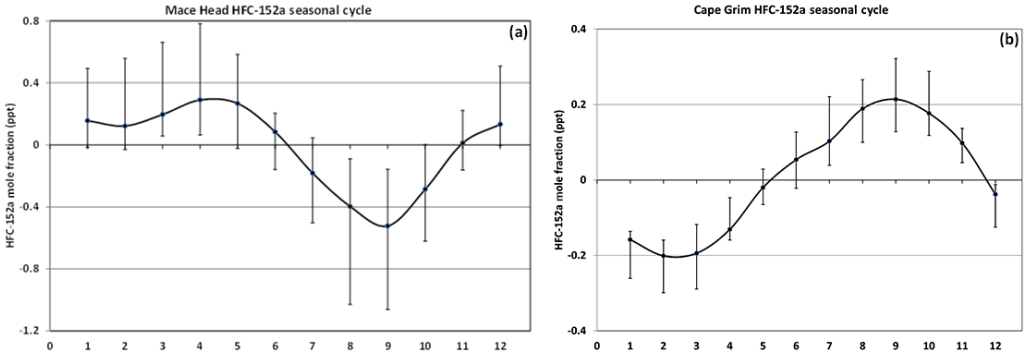


**Figure 5. (a)** Average seasonal cycle at Mace Head, Ireland (2004–2014). Black line represents the average for each month of these individual years and the error bars represent the min to max range. **(b)** Average seasonal cycle at Cape Grim, Tasmania (2004–2014). Black line represents the average for each month of these individual years and the error bars represent the min to max range.

and Europe contribute emissions of $\sim 7$ and $\sim 6\,\mathrm{Gg\,yr^{-1}}$, respectively to the global total. The 2007–2009 North American emission estimate of $28\,\mathrm{Gg\,yr^{-1}}$ agrees within the uncertainties of HFC-152a emission estimates reported in Barletta et al. (2011) and Simmonds et al. (2015). The North American estimate indicates one reason why the UNFCCC reported amount appears to be so low; more than half the global emissions appear to come from this continental region, yet the UNFCCC reports do not include specific HFC-152a emissions from the US.

### 5.2.1 InTEM northwestern Europe (NWEU) estimated emissions from Mace Head observations

The HFC-152a perturbations above baseline, observed at Mace Head, are driven by emissions on regional scales that have yet to be fully mixed on the hemisphere scale. The Mace Head observations are coupled with NAME model air history maps using the inversion system InTEM to estimate surface emissions across NWEU (Manning et al., 2011). NWEU is defined as United Kingdom, Ireland, Germany, France, Benelux, and Denmark.

As shown in Fig. 8, the NWEU emission estimates for HFC-152a from InTEM (rolling 3-yr averages) agree to within inversion uncertainties with the UNFCCC data (2013 submission) for most years. The estimates of NWEU emissions grew steadily from 1995 reaching a maximum emission of $1.6 \pm 0.21\,\mathrm{Gg\,yr^{-1}}$ in 2003 with a subsequent decline to $0.98 \pm 0.34\,\mathrm{Gg\,yr^{-1}}$ in 2013.

### 5.2.2 European estimated emissions from European observations at Mace Head Jungfraujoch and Mt. Cimone

The temporal evolution of emission estimates for different European regions are given in Fig. 9. In contrast to the InTEM estimates the Bayesian inversion derived emissions in NWEU were slightly smaller than the UNFCCC estimate and showed a continued decrease until 2014. Total emissions in the inversion domain ranged from $4 \pm 0.5\,\mathrm{Gg\,yr^{-1}}$ ($2\sigma$ confidence range) for 2006 to only $2.5 \pm 0.2\,\mathrm{Gg\,yr^{-1}}$ in 2014. This is considerably smaller than the European Annex I estimate given in Sect. 5.2, but covers a significantly smaller geographical region. The estimate given in Sect. 5.2 encompassed all countries in Europe extending beyond the bounds

**Table 3.** Annex 1 and non-Annex 1 global and regional emissions in Gg yr$^{-1}$ averaged over two 3-year periods. Values in the final column are from the 12-box model, all other values are from the combined Eulerian and Lagrangian model of Lunt et al. (2015). The global estimates from the 12-box model are not in exact agreement with the combined Annex I and non-Annex I emissions reported in Lunt et al. 2015. However, this is not unexpected, given the vastly different transport and inversion models used to estimate these terms. We note that the uncertainty range of the combined Annex I and non-Annex I estimates does overlap with the uncertainty range from the 12-box model, and a similar growth in emissions is seen across the two averaging periods.

| 3-year Averages | Europe | North America | East Asia | East Asia | GLOBAL | GLOBAL | GLOBAL |
|---|---|---|---|---|---|---|---|
| Annex 1 | Annex 1 | Annex 1 | Non-Annex 1 | Annex 1 | Non-Annex 1 | 12-box model | |
| 2007–2009 | 6.4 (5.2–7.5) | 28.0 (22.5–33.4) | 0.4 (0.2–1.2) | 5.8 (4.5–7.5) | 35.2 (27.7–42.6) | 6.6 (4.3–9.2) | 48.5 (37.0–60.6) |
| 2010–2012 | 5.2 (4.1–6.4) | 31.6 (24.5–38.6) | 1.0 (0.5–1.6) | 6.0 (4.3–8.2) | 40.2 (31.3–49.3) | 6.6 (3.9–9.8) | 53.9 (43.0–67.3) |

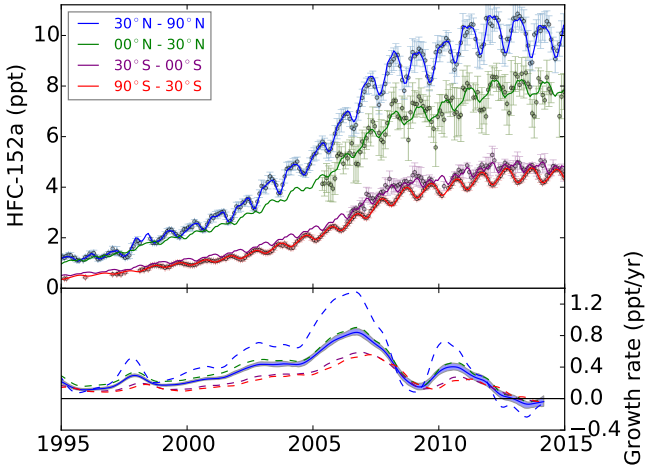


**Figure 6.** Top panel: AGAGE 12-box model mole fractions (solid line) for the two NH (30–90° N, MHD, and THD and 00–30° N, RGP) and the two SH (30–00° S, SMO and 90–30° S, CGO) latitudinal bands The points show the semi-hemispheric monthly mean observations from the five AGAGE stations used in the inversion (MHD, THD, RPB, SMO, CGO). Lower panel: HFC-152a semi-hemisphere annualized growth rates are shown as dashed lines (see Rigby et al., 2014 for smoothing method), with the solid blue line and shading showing the global mean and its uncertainty.

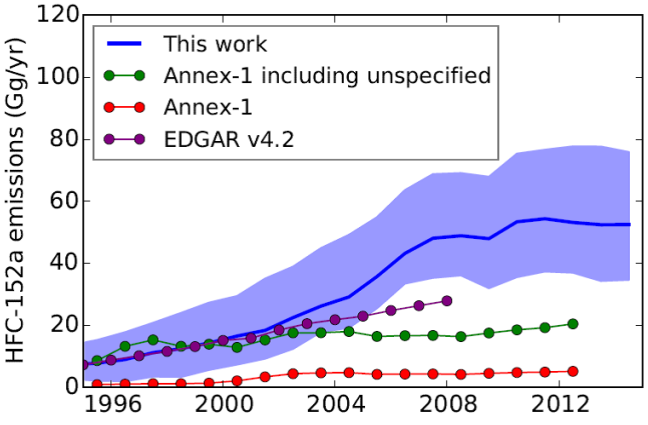


**Figure 7.** HFC-152a emissions estimates derived from observations (blue line and shading, 1$\sigma$ uncertainty) and inventories. The purple line shows the global emissions estimates from EDGAR (v4.2), the red line shows the emissions reported to the UNFCCC and the green line shows emissions calculated from all data reported to UNFCCC, including allowance for the HFC-152a component of unspecified emissions.

of the area indicated in Fig. 1 (red box). The steady decline in emissions was interrupted by a local maximum in the years 2010–2012, when emissions reached $3.6 \pm 0.5$ (Gg yr$^{-1}$). A minimum in the posterior emissions can be seen in 2009 and was most pronounced for the Iberian Peninsula, Italy, France and Germany, which might indicate the influence of the European recession in 2008–2009. For NWEU the emission estimate remains slightly below the UNFCCC estimates and those estimated by InTEM, but support the declining trend in European emissions. Despite the fact that Italy does not report HFC-152a emissions to the UNFCCC, the largest by country emissions were estimated for Italy (up to 1 Gg yr$^{-1}$ in 2007). However, a strong decline in these emissions after 2011 was established here. Similar values for Italian HFC-152a emissions were reported by Brunner et al. (2012) using observations from Jungfraujoch and Mace Head (but not Mt. Cimone) in an extended Kalman Filter inversion.

### 5.2.3 US estimated emissions

Estimates of North American emissions have been reported by several groups (see also estimates from this study in Table 3). Millet et al. (2009) report average US emissions for 2004–2006 of 7.6 Gg (4.8–10 Gg) compared with the UNFCCC average 2005–2006 estimate of 12.3 Gg calculated from UNFCCC data. Miller et al. (2012) provided HFC-152a emissions estimates averaged from 2004–2009 of 25 Gg (11–50 Gg). Barletta et al. (2011) reported a 2008 HFC-152a emission estimate of $32 \pm 4$ Gg. In a recent investigation of the surface-to-surface transport of HFC-152a from North America to Mace Head, Ireland, an interspecies correlation method with HFC-125 as the reference gas was also used to

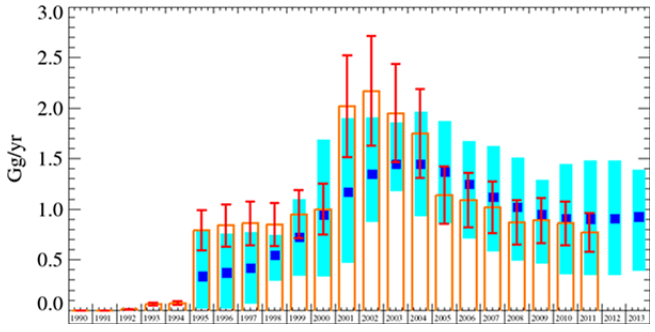


**Figure 8.** Emission (Gg yr$^{-1}$) estimates for HFC-152a from northwestern Europe. The blue uncertainty bars represent the 5th and 95th percentiles of the InTEM estimates (rolling 3-yr averages). The orange bars and associated uncertainty are the UNFCCC inventory estimates for the NWEU region. (25 % uncertainty is estimated by the UK in their National Inventory Report (NIR) submission to the UNFCCC, the same uncertainty was assumed for northwestern Europe given the lack of additional information).

estimate North American emissions primarily from the eastern seaboard region. The average 2008 HFC-152a emission estimate was $31.3 \pm 5.9$ Gg (Simmonds et al., 2015); in very close agreement with the estimate from Barletta et al. (2011). HFC-152a emission estimates for 2005 (10.1 Gg) and 2006 (12.5 Gg) reported by Stohl et al. (2009) are close to the (recalculated) UNFCCC estimates in those years.

If the sources of emissions from the US were solely technical aerosols and construction foam, emissions would be expected to be far lower. These were the historic uses in Europe and Japan and resulted in emissions 10 times less than those estimated for the US. However, in the US, do-it-yourself (DIY) refilling of car air conditioners is not only permitted but thriving (Zhan et al., 2014), with an estimated 24 million DIY refilling operations attempted each year. The practice is banned in Europe (OJ, 2014).

Furthermore, there is ample evidence online that HFC-152a is extensively used in DIY refilling on account of its lower cost. It is a technically suitable replacement for HFC-134a, although there are safety concerns of importance to vehicle manufacturers (Hill, 2003). If the quantities estimated by Zhan et al. (2014) were met using HFC-152a diverted from the retail trade in technical aerosols, some 10 to 20 Gg yr$^{-1}$ of HFC-152a could be released into the atmosphere from this source alone.

#### 5.2.4 East Asian emissions

Emissions of HFC-152a from China were estimated to be $4.3 \pm 2.3$ Gg yr$^{-1}$ in 2004–2005 (Yokouchi et al., 2006), $3.4 \pm 0.5$ Gg yr$^{-1}$ in 2008 (Stohl et al., 2010) and 5.7 (4.3–7.6) Gg yr$^{-1}$ in 2008 (Kim et al., 2010). Li et al. (2011) using an interspecies correlation method also reported emission estimates for East Asia (China, South Korea, and Taiwan, with HCFC-22 as the reference tracer) and Japan (reference tracer HFC-134a) for the period between November 2007 and December 2008. For China, emissions were estimated to be 5.4 (4–7.4) Gg yr$^{-1}$. In contrast, the Taiwan region, Korea, and Japan had lower estimated emissions totalling 1.39 Gg yr$^{-1}$. These estimates are within the uncertainties of our East Asia emissions reported in Sect. 5.2 and Table 3.

Yao et al. (2012), using the interspecies correlation method with carbon monoxide as the reference tracer, reported more recent Chinese emissions of $2 \pm 1.8$ Gg yr$^{-1}$ in 2010–2011. This would imply some reduction in Chinese emissions compared with earlier years.

#### 5.2.5 Australian HFC-152a emissions from Cape Grim data

SE Australian emissions of HFC-152a are estimated using the positive enhancements above baseline or background concentrations observed at Cape Grim using interspecies correlation with CO as the reference species (ISC: Dunse et al., 2005; Greally et al., 2007) and inverse modeling (InTEM: Manning et al., 2003, 2011). Figure 2a (CGO) shows an overall increase in the magnitude of HFC-152a pollution episodes, presumably due to increasing regional emissions. Detailed analysis of these pollution episodes using air mass back trajectories shows clearly that the HFC-152a pollution seen at Cape Grim originates largely from Melbourne and the surrounding Port Phillip region.

Australian HFC-152a emissions of 5–10 Mg yr$^{-1}$ via interspecies correlation (ISC) have been reported for the period 1998–2004, although it was noted that these emission estimates were near the detection limit of the ISC method (Greally et al., 2007). Recently, significant improvements have been made to this ISC method, including a revised (upward) CO emissions inventory for the Melbourne/Port Phillip region, exclusion of high CO events in the Cape Grim in situ CO record, resulting from CO emissions from biomass burning and coal combustion in the Latrobe Valley (east of Port Phillip) and a revised (upward) population-based scaling factor (5.4), used to convert Melbourne/Port Phillip emissions to Australian emissions (Fraser et al., 2014a, b). Each of these changes to the ISC method resulted in higher trace gas emission estimates. The revised (compared to Greally et al., 2007) Australian HFC-152a emission estimates from the ISC method are shown in the 2nd column of Table 4 and in Fig. 10 as 3-year running averages.

The InTEM model (Manning et al., 2003, 2011) has been used to derive HFC-152a emissions from Victoria/Tasmania (Fraser et al., 2014a). Annual Australian emissions are calculated from Victoria/Tasmania emissions using a population based scale factor of 3.7 and are shown in Fig. 10 and the 3rd column of Table 4, interpolated from rolling 3-year emission estimates. Over the period 2002–2011, the average Australian HFC-152a emissions from ISC and InTEM agree to within 2 %. The method for estimating the InTEM uncertainties are discussed above. No additional uncertainty was

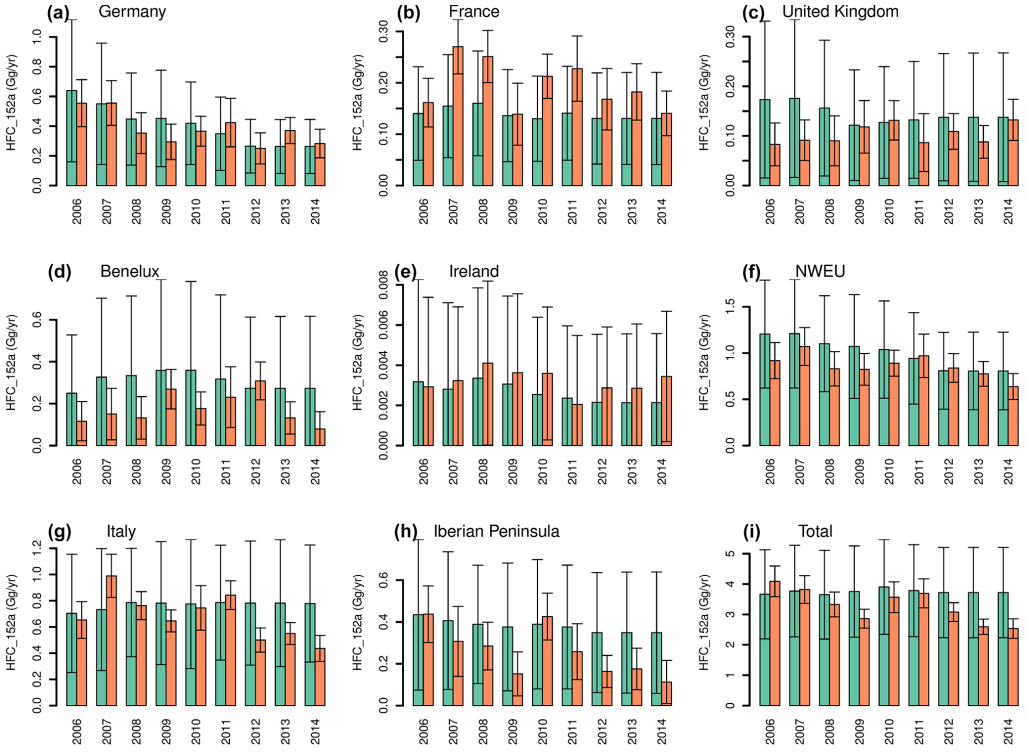


**Figure 9.** HFC-152a emission estimates for different European regions using the Bayesian regional inversion (orange bars) and prior estimates as reported to UNFCCC (green bars). Error bars indicate $2\sigma$ confidence levels. Total prior uncertainties were set to 20 % of the total domain emissions, which may result in different levels of relative uncertainty for each country/region. Note that prior estimates for Italy were taken from EDGAR instead. Prior values for 2012 were repeated for each region after 2012.

**Table 4.** Australian HFC-152a emissions (Mg $yr^{-1}$, 3-year running averages) calculated from Cape Grim in situ observations via ISC (ADS and Medusa data, uncertainty: ±1 SD) and inverse modeling using InTEM (Medusa data, range: 25th–75th percentiles); ISC, NAME averages weighted by uncertainties, ISC InTEM average for 2004 is based only on InTEM data.

| YEAR | ISC | InTEM | ISC and InTEM average | ISC / InTEM ratio |
|---|---|---|---|---|
| 1999 | 24 ± 7 | | | |
| 2000 | 25 ± 8 | | | |
| 2001 | 27 ± 9 | | | |
| 2002 | 28 ± 10 | 32 (31–34) | 31 ± 2 | |
| 2003 | 28 ± 10 | 32 (29–33) | 31 ± 4 | 0.88 |
| 2004 | 29 ± 10 | 31 (29–33) | 31 ± 2 | 0.94 |
| 2005 | 32 ± 10 | 31(30–33) | 31 ± 4 | 1.03 |
| 2006 | 38 ± 10 | 35 (32–38) | 35 ± 6 | 1.09 |
| 2007 | 51 ± 15 | 41 (37–43) | 42 ± 6 | 1.24 |
| 2008 | 49 ± 15 | 43 (41–47) | 44 ± 5 | 1.14 |
| 2009 | 52 ± 15 | 68 (64–72) | 65 ± 8 | 0.76 |
| 2010 | 59 ± 20 | 69 (64–74) | 67 ± 10 | 0.86 |
| 2011 | 56 ± 15 | 72 (68–76) | 69 ± 7 | 0.78 |
| 2012 | 77 ± 25 | | | |
| 2013 | 69 ± 24 | | | |

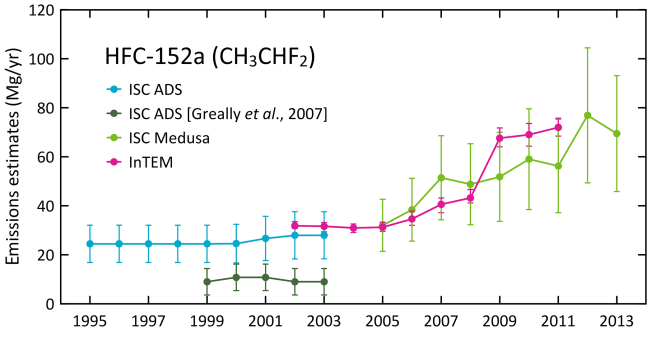


**Figure 10.** Australian HFC-152a emissions ($Mg\,yr^{-1}$) calculated from Cape Grim in situ observations via ISC, using ADS and Medusa data, and inverse modeling using InTEM (Medusa data). Australian emissions are derived from SE Australian emissions, scaled by population (see text). Uncertainties are 25th–75th percentiles (InTEM) and 1 SD (ISC).

applied to the estimates through the process of up-scaling from Victoria/Tasmania to Australian totals. The assumption was made that the use of HFC-152a per head of population was identical across Australia as we have no more detailed information.

Australian HFC-152a emissions have increased steadily from 25 $Mg\,yr^{-1}$ in the late-1990s to over 60 $Mg\,yr^{-1}$ in the late-2000s. The 2012 and 2013 emissions have been estimated from Cape Grim data by ISC at 77 and 69 Mg, respectively. Australian HFC-152a emissions (1998–2004) are 25–30 Mg, significantly higher than estimated (5–10 $Mg\,yr^{-1}$) in Greally et al. (2007), resulting from improvements in the ISC method (see above).

Compared to the global values derived above, Australian emissions are 0.1 % of global emissions based on ISC/InTEM data. It is unusual for Australian emissions of an industrial chemical to be as low as 0.1 % of global emissions. For other HFCs, CFCs and HCFCs (for example HFC-134a, CFC-12, HCFC-22), Australian emissions as fraction of global emissions are typically 1–2 %, similar to Australia's fraction of global gross domestic product (GDP, 1.9 %, 2014) but significantly larger than Australia's fraction of global population (0.33 %, 2014) (Fraser et al., 2014b).

The possible reasons for the low Australian HFC-152a emissions (relatively low use in Australia compared to rest of world) are being investigated. One suggestion (M. Bennett, Refrigerant Reclaim Australia, personal communication, 2013) is that a significant major-volume use in other parts of the world for HFC-152a is as an aerosol propellant, a use not taken up to any significant degree in Australia.

## 6 Conclusions

Atmospheric abundances and temporal trends of HFC-152a have been estimated from data collected at the network of 11 globally distributed monitoring sites. The longest continuous in situ record at Mace Head, Ireland covers a 20-year period from 1994–2014. Other stations within the network have observational records from 9 to 16 years, with only a short record (2010–2012) at Shangdianzi, China. From selected baseline in situ measurements and measurements of archived air samples dating back to 1978 the long-term growth rate of HFC-152a has been deduced. Analyzing the enhancements above baseline coupled with atmospheric transport models permitted us to estimate both regional and global HFC-152a emissions. However, it should be noted that the various models use different domains to obtain regional emissions estimates.

The annual average NH (Mace Head + Trinidad Head) baseline mole fraction in 1994 was 1.2 ppt reaching an annual average mole fraction of 10.1 ppt in 2014. In the SH (Cape Grim) the annual average mole fraction increased from 0.84 ppt in 1998 to 4.5 ppt in 2014. Using the global average mole fraction obtained from the AGAGE 12-box model we estimate that the HFC-152a contribution to radiative forcing was $0.61 \pm 0.02\,mW\,m^{-2}$ in 2014. Since the first in situ measurements in 1994 the global annual growth rate of HFC-152a has increased to a maximum annual growth rate in 2006 of $0.84 \pm 0.05\,ppt\,yr^{-1}$. More recently the average annual growth rate has slowed to $0.38 \pm 0.04\,ppt\,yr^{-1}$ in 2010, and become negative, with a growth rate in 2013–2014 of minus $0.06 \pm 0.05\,ppt\,yr^{-1}$.

Global HFC-152a emissions increased from $7.3 \pm 5.6\,Gg\,yr^{-1}$ in 1994 to $52.5 \pm 20.15\,Gg\,yr^{-1}$ in 2014. Global emissions are dominated by emissions from North America with this region being responsible for ∼ 67 % of global emissions in our estimates. Estimates of northwest European emissions of $\sim 0.9\,Gg\,yr^{-1}$, (2010–2012 average) agree within the uncertainties for the two regional models (see Sect. 3.3 and 3.4) and overlap with the UNFCCC inventory. For the combined Eulerian and Lagrangian models (see Sect. 3.2 and Table 3) that encompass all European countries, we derive a 2010–2012 average emission of $5.2\,Gg\,yr^{-1}$. East Asian countries contribute $1\,Gg\,yr^{-1}$ (Annex 1) and $6\,Gg\,yr^{-1}$ (Non-Annex 1) to the global total (2010–2012 averages). All of the models studies indicate a current declining trend in European and Asian emissions.

Substantial differences in emission estimates of HFC-152a were found between this study and those reported to the UNFCCC which we suggest arises from underestimated North American emissions and undeclared Asian emissions; reflecting the incomplete global reporting of GHG emissions to the UNFCCC and/or biases in the accounting methodology. Ongoing, continuous, and accurate globally and regionally distributed atmospheric measurements of GHGs, such as HFC-152a, are required for "top-down" quantification of global and regional emissions of these gases, thereby enabling improvements in national emissions inventories, or "bottom-up" emissions data collected and reported to the UNFCCC (Weiss and Prinn, 2011).

## Data availability

The entire ALE/GAGE/AGAGE data base comprising every calibrated measurement including pollution events is archived on the Carbon Dioxide Information and Analysis Center (CDIAC) at the US Department of Energy, Oak Ridge National Laboratory.

*Acknowledgements.* We specifically acknowledge the cooperation and efforts of the station operators (G. Spain, MHD; R. Dickau, THD; P. Sealy, RPB; NOAA officer-in-charge, SMO) at the AGAGE stations and all other station managers and support staff at the different monitoring sites used in this study. We particularly thank NOAA and NILU for supplying some of the archived air samples shown, allowing us to fill important gaps. The operation of the AGAGE stations was supported by the National Aeronautic and Space Administration (NASA, USA) (grants NAG5-12669, NNX07AE89G and NNX11AF17G to MIT; grants NAG5-4023, NNX07AE87G, NNX07AF09G, NNX11AF15G and NNX11AF16G to SIO); the Department of the Energy and Climate Change (DECC, UK) (contract GA0201 to the University of Bristol); the National Oceanic and Atmospheric Administration (NOAA, USA) (contract RA133R09CN0062 in addition to the operations of American Samoa station); and the Commonwealth Scientific and Industrial Research Organisation (CSIRO, Australia), Bureau of Meteorology (Australia). Financial support for the Jungfraujoch measurements is acknowledged from the Swiss national programme HALCLIM (Swiss Federal Office for the Environment (FOEN)). Support for the Jungfraujoch station was provided by International Foundation High Altitude Research Stations Jungfraujoch and Gornergrat (HFSJG). The measurements at Gosan, South Korea were supported by the Basic Science Research Program through the National Research Foundation of Korea (NRF) funded by the Ministry of Science, ICT & Future Planning (2014R1A1A3051944). Financial support for the Zeppelin measurements is acknowledged from the Norwegian Environment Agency. Financial support for the Shangdianzi measurements is acknowledged from the National Nature Science Foundation of China (41030107, 41205094). The CSIRO and the Australian Government Bureau of Meteorology are thanked for their ongoing long-term support of the Cape Grim station and the Cape Grim science program. M. Rigby is supported by a NERC Advanced Fellowship NE/I021365/1.

Edited by: E. Harris

## References

Archibald, A. T., Witham, C. S., Ashfold, M. J., Manning, A. J., O'Doherty, S., Greally, B. R., Young, D., and Shallcross D. E.: Long-term high frequency measurements of ethane, benzene and methyl chloride at Ragged Point, Barbados: Identification of long-range transport events, Elementa: Science of the Anthropocene, 3, 000068, doi:10.12952/journal.elementa.000068, 2015.

Arnold, T., Mühle, J., Salameh, P. K., Harth, C. M., Ivy, D. J., and Weiss, R. F.: Automated measurement of nitrogen trifluoride in ambient air, Anal. Chem., 84, 4798–4804, 2012.

Ashford, P., Clodic, D., McCulloch, A., and Kuijpers, L.: Emission profiles from the foam and refrigeration sectors comparison with atmospheric concentrations. Part 2: Results and discussion, Int. J. Refrigeration, 27, 701–716, 2004.

Barletta, B., Nissenson, P., Meinardi, S., Dabdub, D., Sherwood Rowland, F., VanCuren, R. A., Pederson, J., Diskin, G. S., and Blake, D. R.: HFC-152a and HFC-134a emission estimates and characterization of CFCs, CFC replacements, and other halogenated solvents measured during the 2008 ARCTAS campaign (CARB phase) over the South Coast Air Basin of California, Atmos. Chem. Phys., 11, 2655–2669, doi:10.5194/acp-11-2655-2011, 2011.

Brunner, D., Henne, S., Keller, C. A., Reimann, S., Vollmer, M. K., O'Doherty, S., and Maione, M.: An extended Kalman-filter for regional scale inverse emission estimation, Atmos. Chem. Phys., 12, 3455–3478, doi:10.5194/acp-12-3455-2012, 2012.

Cunnold, D. M., Prinn, R. G., Rasmussen, R., Simmonds, P. G., Alyea, F. N., Cardlino, C., Crawford, A. J., Fraser, P. J., and Rosen, R.: The lifetime atmospheric experiment, III: lifetime methodology and application to three years of $CFCl_3$ data, J. Geophys. Res., 88, 8379–8400, 1983.

Cunnold, D. M., Fraser, P. J., Weiss, R. F., Prinn, R. G., Simmonds, P. G., Miller, B. R., Alyea, F. N., Crawford, A. J., and Rosen, R.: Global trends and annual releases of $CCl_3F$ and $CCl_2F_2$ estimated from ALE/GAGE and other measurements from July 1978 to June 1991, J. Geophys. Res., 99, 1107–1126, 1994.

DoE: National Inventory Report 2012, Volume 1, Australian Government Department of the Environment, April 2014, 351 pp., 2014.

Dunse, B.: Investigation of urban emissions of trace gases by use of atmospheric measurements and a high-resolution atmospheric transport model. PhD thesis, Wollongong University, Wollongong, NSW, Australia, 2002.

Dunse, B., Steele, P., Fraser, P., and Wilson, S.: An analysis of Melbourne pollution episodes observed at Cape Grim from 1995–1998, in: Baseline Atmospheric Program (Australia) 1997–98, edited by: Tindale, N., Francey, R., and Derek, N., Bureau of Meteorology and CSIRO Atmospheric Research, Melbourne, Australia, 34–42, 2001.

Dunse, B., Steele, P., Wilson, S., Fraser, P., and Krummel, P.: Trace gas emissions from Melbourne Australia, based on AGAGE observations at Cape Grim, Tasmania, 1995–2000, Atmos. Environ., 39, 6334–6344, 2005.

EC-JRC/PBL.: Emission Database for Global Atmospheric Research (EDGAR), version 4.2, European Commission, Joint Research Centre (JRC)/Netherlands Environmental Assessment Agency (PBL), available at: http://edgar.jrc.ec.europa.eu (last access: 1 March 2015), 2011.

Emmons, L. K., Walters, S., Hess, P. G., Lamarque, J.-F., Pfister, G. G., Fillmore, D., Granier, C., Guenther, A., Kinnison, D., Laepple, T., Orlando, J., Tie, X., Tyndall, G., Wiedinmyer, C., Baughcum, S. L., and Kloster, S.: Description and evaluation of the Model for Ozone and Related chemical Tracers, version 4 (MOZART-4), Geosci. Model Dev., 3, 43–67, doi:10.5194/gmd-3-43-2010, 2010.

Forster, P., Ramaswamy, V., Artaxo, P., Berntsen, T., Betts, R., Fahey, D. W., Haywood, J., Lean, J., Lowe, D. C., Myhre, G., Nganga, J., Prinn, R., Raga, G., Schulz, M., and Van Dorland, R.: Changes in atmospheric constituents and in radiative forcing, in: Climate Change (2007): The Physical Science Basis. Contribution of Working Group I to the Fourth Assessment Report of the Intergovernmental Panel on Climate Change, edited by: Solomon, S., 2007.

Fraser, P., Dunse, B., Krummel, P., Steele, P., and Derek, N., Australian HFC, PFC, Sulphur Hexafluoride & Sulphuryl Fluoride Emissions, Australian Government Department of the Environment, 28 pp., 2014a.

Fraser, P., Dunse, B., Manning, A. J., Wang, R., Krummel, P., Steele, P., Porter, L., Allison, C., O'Doherty, S., Simmonds, P., Mühle, J., and Prinn, R.: Australian carbon tetrachloride ($CCl_4$) emissions in a global context, Environ. Chem., 11, 77–88, 2014b.

Ganesan, A. L., Rigby, M., Zammit-Mangion, A., Manning, A. J., Prinn, R. G., Fraser, P. J., Harth, C. M., Kim, K.-R., Krummel, P. B., Li, S., Mühle, J., O'Doherty, S. J., Park, S., Salameh, P. K., Steele, L. P., and Weiss, R. F.: Characterization of uncertainties in atmospheric trace gas inversions using hierarchical Bayesian methods, Atmos. Chem. Phys., 14, 3855–3864, doi:10.5194/acp-14-3855-2014, 2014.

Greally, B. R., Manning, A. J., Reimann, S., McCulloch, A., Huang, J., Dunse, B. L., Simmonds, P. G., Prinn, R. G., Fraser, P. J., Cunnold, D. M., O'Doherty, S., Porter, L. W., Stemmler, K., Vollmer, M. K., Lunder, C. R., Schmidbauer, N., Hermansen, O., Arduini, J., Salameh, P. K., Krummel, P. B., Wang, R. H. J., Folini, D., Weiss, R. F., Maione, M., Nickless, G., Stordal, F., and Derwent, R. G.: Observations of 1,1-difluoroethane (HFC-152a) at AGAGE and SOGE monitoring stations in 1994–2004 and derived global and regional emission estimates, J. Geophys. Res., 112, D06308, doi:10.1029/2006JD007527, 2007.

Hill, W. R.: HFC152a as the alternative refrigerant, available at: http://ec.europa.eu/environment/archives/mac2003/pdf/hill.pdf (last access: 1 March 2015), 2003.

IPCC/TEAP: Progress Report-Volume-1-May 2011. Technology and Assessment Panel. United Nations Environment Programme, Ozone Secretariat, P.O. Box 30552, Nairobi, Kenya, 2011.

Keller, C. A., Hill, M., Vollmer, M. K., Henne, S., Brunner, D., Reimann, S., O'Doherty, S., Arduini, J., Maione, M., Ferenczi, Z., Haszpra, L., Manning, A. J., and Peter, T.: European Emissions of Halogenated Greenhouse Gases Inferred from Atmospheric Measurements, Environ. Sci. Technol., 46, 217–225, doi:10.1021/es202453j, 2012.

Kim, J., Li, S., Kim, K.-R., Stohl, A., Mühle, J., Kim, S.-K., Park, M.-K., Kang, D.-J., Lee, G., Harth, C. M., Salameh, P. K., and Weiss, R. F.: Regional emissions determined from measurements at Jeju Island, Korea: Halogenated compounds from China. Geophys. Res. Lett, 37, L12801, doi:10.1029/2010GL043263, 2010.

Krummel, P. B., Langenfelds, R. L., Fraser, P. J., Steele, L. P., and Porter, L. W.: Archiving of Cape Grim air, in Baseline Atmospheric Program, Australia 2005–2006, edited by: Cainey, J. M., Derek, N., and Krummel, P. B., Australian Bureau of Meteorology and CSIRO Marine and Atmospheric Research, Melbourne, Australia, 55–57, 2007.

Krummel, P. B., Fraser, P. Steele, P., Derek, N., Rickard, C., Ward, J., Somerville, N., Cleland, S., Dunse, B., Langenfelds, R., Baly S., and Leist, M.: The AGAGE in situ program for non-$CO_2$ greenhouse gases at Cape Grim, 2009–2010, Baseline Atmospheric Program (Australia) 2009–2010, edited by: Krummel, N. D. P. and Cleland, S., Australian Bureau of Meteorology and CSIRO Marine and Atmospheric Research, Melbourne, Australia, 55–70, 2014.

Langenfelds, R. L., Fraser, P. J., Francey, R. J., Steele, L. P., Porter, L. W., and Allison, C. E.: The Cape Grim Air Archive; the first seventeen years, 1978–1995, in: Baseline Atmospheric Program, Australia 1994–1995, edited by: Francey, R. J., Dick, A. L., and Derek, N., Bureau of Meteorology and CSIRO Division of Atmospheric Research, Melbourne, 53–70, 1996.

Li, S., Kim, J., Kim, K.-R., Mühle, J., Kim, S.-K., Park, M.-K., Stohl, A., Kang, D.-J., Arnold, T., Harth, C. M., Salameh, P. K., and Weiss, R. F.: Emissions of halogenated compounds in East Asia determined from measurements at Jeju Island, Korea, Environ. Sci. Technol., 45, 5668–5675, doi:10.1021/es104124k, 2011.

Lunt, M. F., Rigby, M., Ganesan, A. L., Manning, A. J., Prinn, R. G., O'Doherty, S., Mühle, J., Harth, C. M., Salameh, P. K., Arnold, T., Weiss, R. F., Saito, T., Yokouchi. Y., Krummel, P. B., Steele, L. P., Fraser, P. J., Li, S., Park, S., Reimann, S., Vollmer, M. K., Lunder, C., Hermansen, O., Schmidbauer, N., Maione, M., Young, D., and Simmonds, P. G.: Reconciling reported and unreported HFC emissions with atmospheric observations, Proc. Natl. Acad. Sci., 112, 5927–5931, doi:10.1073/pnas.1420247112, 2015.

Maione, M., Graziosi, F., Arduini, J., Furlani, F., Giostra, U., Blake, D. R., Bonasoni, P., Fang, X., Montzka, S. A., O'Doherty, S. J., Reimann, S., Stohl, A., and Vollmer, M. K.: Estimates of European emissions of methyl chloroform using a Bayesian inversion method, Atmos. Chem. Phys., 14, 9755–9770, doi:10.5194/acp-14-9755-2014, 2014.

Manning, A. J. and Weiss, R. F.: Quantifying Regional GHG Emissions from Atmospheric Measurements: HFC-134a at Trinidad Head, 50th anniversary of the Global Carbon Dioxide Record Symposium and Celebration, Kona, Hawaii, available at: http:///www.esrl.noaa.gov/gmd/co_2_conference/pdfs/quantifying_abstract.pdf (last access: July 2010), 2007.

Manning, A. J., Ryall, D., Derwent, R., Simmonds, P., and O'Doherty, S.: Estimating European ozone depleting and greenhouse gases using observations and a modelling attribution technique, J. Geophys. Res., 108, 4405, doi:10.1029/2002JD002312, 2003.

Manning, A. J., O'Doherty, S., Jones, A. R., Simmonds, P. G., and Derwent, R. G.: Estimating UK methane and nitrous oxide emissions from 1990 to 2007 using an inversion modelling approach, J. Geophys. Res., 116, D02305, doi:1029/2010JD014763, 2011.

McCulloch, A.: Evidence for improvements in containment of fluorinated hydrocarbons during use: an analysis of reported European emissions, Environ. Sci. Policy., 12, 149–156, doi:10.1016/j.envsci.2008.12.003, 2009.

Miller, B., Weiss, R., Salameh, P., Tanhua, T., Greally, B., Muhle, J., and Simmonds, P.: Medusa: a sample pre-concentration and GC-MS detector system for *in situ* measurements of atmospheric trace halocarbons, hydrocarbons and sulphur compounds, Anal. Chem., 80, 1536–1545, 2008.

Miller, B. R., Rigby, M., Kuijpers, L. J. M., Krummel, P. B., Steele, L. P., Leist, M., Fraser, P. J., McCulloch, A., Harth, C., Salameh, P., Mühle, J., Weiss, R. F., Prinn, R. G., Wang, R. H.

J., O'Doherty, S., Greally, B. R., and Simmonds, P. G.: HFC-23 (CHF3) emission trend response to HCFC-22 (CHClF2) production and recent HFC-23 emission abatement measures, Atmos. Chem. Phys., 10, 7875–7890, doi:10.5194/acp-10-7875-2010, 2010.

Miller, J. B., Lehman, S. J., Montzka, S. A., Sweeney, C., Miller, B. R., Karion, A., Wolak, C., Dlugokencky, E. J., Southon, J., Turnbull, J. C., and Tans, P. P.: Linking emissions of fossil fuel $CO_2$ and other anthropogenic trace gases using atmospheric $^{14}CO_2$, J. Geophys. Res., 117, D08302, doi:10.1029/2011JD017048, 2012.

Millet, D. B., Atlas, L. E., Blake, D. R., Blake, N. J., Diskin, C. S., Holloway, J. D., Hudman, R. C., Meinardi, S., Ryerson, T. B., and Sachse, G. W.: Halocarbon emissions from the United States and Mexico and their Global warming potential. Environ. Sci. Technol., 43, 1055–1060, doi:10.1021/Es802146j, 2009.

Mühle, J., Ganesan, A. L., Miller, B. R., Salameh, P. K., Harth, C. M., Greally, B. R., Rigby, M., Porter, L. W., Steele, L. P., Trudinger, C. M., Krummel, P. B., O'Doherty, S., Fraser, P. J., Simmonds, P. G., Prinn, R. G., and Weiss, R. F.: Perfluorocarbons in the global atmosphere: tetrafluoromethane, hexafluoroethane, and octafluoropropane, Atmos. Chem. Phys., 10, 5145–5164, doi:10.5194/acp-10-5145-2010, 2010.

Myhre, G., Shindell, D., Bréon, F.-M., Collins, W., Fuglestvedt, J., Huang, J., Koch, D., Lamarque, J.-F., Lee, D., Mendoza, B., Nakajima, T., Robock, A., Stephens, G., Takemura, T., and Zhang, H.: Anthropogenic and Natural Radiative Forcing. In: Climate Change 2013: The Physical Science Basis. Contribution of Working Group I to the Fifth Assessment Report of the Intergovernmental Panel on Climate Change, edited by: Stocker, T. F., Qin, D., Plattner, G. K., Tignor, M., Allen, S. K., Boschung, J., Nauels, A., Xia, Y., Bex, V., and Midgley, P. M. Cambridge University Press, Cambridge, United Kingdom and New York, NY, USA, 2013.

O'Doherty, S., Cunnold, D., Sturrock, G. A., Ryall, D., Derwent, R. G., Wang, R. H. J., Simmonds, P., Fraser, P. J., Weiss, R. F., Salameh, P., Miller, B. R., and Prinn, R. G.: In-Situ Chloroform Measurements at AGAGE Atmospheric Research Stations from 1994–1998, J. Geophys. Res., 106, 20429–20444, 2001.

O'Doherty, S., Cunnold, D. M., Miller, B. R., Mühle, J., McCulloch, A., Simmonds, P. G., Mühle, J., McCulloch, A., Simmonds, P. G., Manning, A. J., Reimann, S., Vollmer, M. K., Greally, B. R., Prinn, R. G., Fraser, P. J., Steele, L. P., Krummel, P. B., Dunse, B. L., Porter, L. W., Lunder, C. R., Schmidbauer, N., Hermansen, O., Salameh, P. K., Harth, C. M., Wang, R. H. J., and Weiss, R. F.: Global and regional emissions of HFC-125 ($CHF_2CF_3$) from in situ and air archive atmospheric observations at AGAGE and SOGE observatories, J. Geophys. Res., 114, D23304, doi:10.1029/2009jd012184, 2009.

O'Doherty, S., Rigby, M., Mühle, J., Ivy, D. J., Miller, B. R., Young, D., Simmonds, P. G., Reimann, S., Vollmer, M. K., Krummel, P. B., Fraser, P. J., Steele, L. P., Dunse, B., Salameh, P. K., Harth, C. M., Arnold, T., Weiss, R. F., Kim, J., Park, S., Li, S., Lunder, C., Hermansen, O., Schmidbauer, N., Zhou, L. X., Yao, B., Wang, R. H. J., Manning, A. J., and Prinn, R. G.: Global emissions of HFC-143a ($CH_3CF_3$) and HFC-32 ($CH_2F_2$) from in situ and air archive atmospheric observations, Atmos. Chem. Phys., 14, 9249–9258, doi:10.5194/acp-14-9249-2014, 2014.

OJ (Official Journal of the European Union): Regulation (EU) No 517/2014 of the European Parliament and of the Council of 16 April 2014 on fluorinated greenhouse gases and repealing Regulation (EC) No 842/2006, Official Journal L 150/195, 2014.

Press, W. H., Teukolsky, S. A., Vetterling, W. T., and Flannery, B. P.: Numerical Recipes in Fortran: The art of scientific computing, 2nd Edn., Cambridge University Press, UK, 1992.

Prinn, R., Cunnold, D., Simmonds, P., Alyea, F., Boldi, R., Crawford, A., Fraser, P., Gutzler, D., Hartlet, D., Rose, R., and Rasmussen, R.: Global average concentration and trend for hydroxyl radicals deduced from ALE/GAGE trichloroethane (methyl chloroform) data for 1978–1990, J. Geophys. Res., 97, 2445–2461, 1992.

Prinn, R., Weiss, R. F., Fraser, P., Simmonds, P., Cunnold, D., Alyea, F., O'Doherty, S., Salameh, P., Miller, B., Huang, J., Wang, R., Hartley, D., Harth, C., Steele, P., Sturrock, G., Midgley, P., and McCulloch, A.: A history of chemically and radiatively important gases in air deduced from ALE/GAGE/AGAGE, J. Geophys. Res., 105, 17751–17792, 2000.

Reimann, S., Schaub, D., Stemmler, K., Folini, D., Hill, M., Hofer, P., Buchmann, B., Simmonds, P. G., Greally, B. R., and O'Doherty, S.: Halogenated greenhouse gases at the Swiss High Alpine Site of Jungfraujoch (3580 m asl): Continuous measurements and their use for regional European source allocation, J. Geophys. Res., 109, D05307, doi:10.1029/2003JD003923, 2004.

Rigby, M., Ganesan, A. L., and Prinn, R. G.: Deriving emissions time series from sparse atmospheric mole fractions, J. Geophys. Res., 116, D08306, doi:10.1029/2010JD015401, 2011a.

Rigby, M., Manning, A. J., and Prinn, R. G.: Inversion of long-lived trace gas emissions using combined Eulerian and Lagrangian chemical transport models, Atmos. Chem. Phys., 11, 9887–9898, doi:10.5194/acp-11-9887-2011, 2011b.

Rigby, M., Prinn, R. G., O'Doherty, S., Montzka, S. A., McCulloch, A., Harth, C. M., Mühle, J., Salameh, P. K., Weiss, R. F., Young, D., Simmonds, P. G., Hall, B. D., Dutton, G. S., Nance, D., Mondeel, D. J., Elkins, J. W., Krummel, P. B., Steele, L. P., and Fraser, P. J.: Re-evaluation of the lifetimes of the major CFCs and CH3CCl3 using atmospheric trends, Atmos. Chem. Phys., 13, 2691–2702, doi:10.5194/acp-13-2691-2013, 2013.

Rigby, M., Prinn, R., O'Doherty, S., Miller, B., Ivy, D., Muhle, J., Harth, C., Salameh, P., Arnold, T., Weiss, R., Krummel, P., Steele, P., Fraser, P., Young, D., and Simmonds, P.: Recent and future trends in synthetic greenhouse gas radiative forcing, Geophys. Res. Lett., 41, 2623–2630, 2014.

Ruckstuhl, A. F., Henne, S., Reimann, S., Steinbacher, M., Vollmer, M. K., O'Doherty, S., Buchmann, B., and Hueglin, C.: Robust extraction of baseline signal of atmospheric trace species using local regression, Atmos. Meas. Tech., 5, 2613–2624, doi:10.5194/amt-5-2613-2012, 2012.

Ryall, D. B., Derwent, R. G., Simmonds, P. G., and O'Doherty, S.: Estimating source regions of European emissions of trace gases from observations at Mace Head, Atmos. Environ., 35, 2507–2523, 2001.

Simmonds, P. G., O'Doherty, S., Nickless, G., Sturrock, G. A., Swaby, R., Knight, P., Ricketts, J., Woffenden, G., and Smith, R.: Automated gas chromatographic/mass spectrometer for routine atmospheric field measurements of the CFC replacement compounds, the hydrofluorocarbons and hydrochlorofluorocarbons, Anal. Chem., 67, 717–723, 1995.

Simmonds, P. G., Derwent, R.G., Manning, A. J., McCulloch, A., and O'Doherty, S.: USA emissions estimates of $CH_3CHF_2$,

$CH_2FCF_3$ and $CH_2F_2$ based on in situ observations at Mace Head, Atmos. Environ., 104, 27–38, 2015.

SPARC Report on the Lifetimes of Stratospheric Ozone-Depleting Substances, Their Replacements and Related Species, SPARC Report No. 6, edited by: Ko, M. K. W., Newman, P. A., Reimann, S., and Strahan, S. E., WCRP-15/2013, December 2013.

Stohl, A., Forster, C., Frank, A., Seibert, P., and Wotawa, G.: Technical note: The Lagrangian particle dispersion model FLEXPART version 6.2, Atmos. Chem. Phys., 5, 2461–2474, doi:10.5194/acp-5-2461-2005, 2005.

Stohl, A., Seibert, P., Arduini, J., Eckhardt, S., Fraser, P., Greally, B. R., Lunder, C., Maione, M., Mühle, J., O'Doherty, S., Prinn, R. G., Reimann, S., Saito, T., Schmidbauer, N., Simmonds, P. G., Vollmer, M. K., Weiss, R. F., and Yokouchi, Y.: An analytical inversion method for determining regional and global emissions of greenhouse gases: Sensitivity studies and application to halocarbons, Atmos. Chem. Phys., 9, 1597–1620, doi:10.5194/acp-9-1597-2009, 2009.

Stohl, A., Kim, J., Li, S., O'Doherty, S., Mühle, J., Salameh, P. K., Saito, T., Vollmer, M. K., Wan, D., Weiss, R. F., Yao, B., Yokouchi, Y., and Zhou, L. X.: Hydrochlorofluorocarbon and hydrofluorocarbon emissions in East Asia determined by inverse modeling, Atmos. Chem. Phys., 10, 3545–3560, doi:10.5194/acp-10-3545-2010, 2010.

Sturrock, G. A., Porter, L. W., Fraser, P. J., Derek, N., and Krummel, P. B.: HCFCs, HFCs, halons, minor CFCs and halomethanes-The AGAGE in situ GC-MS program, 1997–1998, and related measurements on flask air samples collected at Cape Grim, in Baseline Program, Australia 1997–1998, edited by: Tindale, N. W., Derek, N., and Francey, R. J., 97–107, Bureau Of Meteorol., Melbourne, 2001.

Vollmer, M. K., Miller, B. R., Rigby, M., Reimann, S., Mühle, J., Krummel, P. B., O'Doherty, S., Jim, J., Rhee, T. S., Weiss, R. F., Fraser, P. J., Simmonds, P. G., Salameh, P. K., Harth, C. M., Wang, R. H. J., Steele, L. P., Young, D., Lunder, C. R., Hermansen, O., Ivy, D., Arnold, T., Schmidbauer, N., Kim, K.-R., Greally, B. G., Hill, M., Leist, M., Wenger, A., and Prinn, R. G.: Atmospheric histories and global emissions of the anthropogenic hydrofluorocarbons HFC-365mfc, HFC-245fa, HFC-227ea, and HFC-236fa, J. Geophys. Res., 116, D08304, doi:10.1029/2010jd015309, 2011.

Weiss, R. F. and Prinn, R. G.: Quantifying greenhouse-gas emissions from atmospheric measurements: a critical reality check for climate legislation, Phil. Trans. R. Soc. A, 369, 1925–1942, doi:10.1098/rsta.2011.0006, 2011.

Yao, B., Vollmer, M. K., Zhou, L. X., Henne, S., Reimann, S., Li, P. C., Wenger, A., and Hill, M.: In-situ measurements of atmospheric hydrofluorocarbons (HFCs) and perfluorocarbons (PFCs) at the Shangdianzi regional background station, China, Atmos. Chem. Phys., 12, 10181–10193, doi:10.5194/acp-12-10181-2012, 2012.

Yokouchi, Y., Inagki T., Yazawa, K., Tamaru, T., Enomoto, T., and Izumi, K.: Estimates of ratios of anthropogenic halocarbon emissions from Japan based on aircraft monitoring over Sagami Bay, Japan, J. Geophys. Res., 110, D06301, doi:10.1029/2004JD005320, 2005.

Yokouchi, Y., Taguchi, S., Saito, T., Tohjima, Y., Tanimoto, H., and Mukai, H.: High frequency measurements of HFCs at a remote site in East Asia and their implications for Chinese emissions. Geophys. Res. Lett., 33, L21814, doi:10.1029/2006GL026403, 2006.

Zhan T., Potts, W., Collins, J. F., and Austin, J.: Inventory and mitigation opportunities for HFC-134a emissions from nonprofessional automotive service, Atmos. Environ., 99, 17–23, 2014.